Non equilibrium anisotropic excitons in atomically thin ReS2

Urban, J. M.; Baranowski, M.; Kuc, A.; Klopotowski, L.; Surrente, A.; Ma, Y.; Wlodarczyk, D.; Suchocki, A.; Ovchinnikov, D.; Heine, T.; Maude, D. K.; Kis, A.; Plochocka, P.;

Originally published:

November 2018

2D Materials 6(2018), 015012

DOI: https://doi.org/10.1088/2053-1583/aae9b9

Non equilibrium anisotropic excitons in atomically thin ReS_2

J. M. Urban,[1,*] M. Baranowski,[1,2,*] A. Kuc,[3,4] Ł. Kłopotowski,[5] A. Surrente,[1] Y. Ma,[3] D. Włodarczyk,[5] A. Suchocki,[5] D. Ovchinnikov,[6] T. Heine,[3,4,7] D. K. Maude,[1] A. Kis,[6] and P. Plochocka[1,†]

[1] *Laboratoire National des Champs Magnétiques Intenses, UPR 3228, CNRS-UGA-UPS-INSA, Grenoble and Toulouse, France*
[2] *Department of Experimental Physics, Faculty of Fundamental Problems of Technology, Wroclaw University of Science and Technology, Wroclaw, Poland*
[3] *Wilhelm-Ostwald Institute für Physikalische und Theoretische Chemie, Universität Leipzig, Linné Str. 2, 04103 Leipzig, Germany*
[4] *Helmholtz-Zentrum Dresden-Rossendorf, Abteilung Ressourcenökologie, Forschungsstelle Leipzig, Permoserstr. 15, 04318, Leipzig, Germany*
[5] *Institute of Physics, Polish Academy of Sciences, Al. Lotników 32/46, 02-668 Warsaw, Poland*
[6] *Electrical Engineering Institute and Institute of Materials Science and Engineering, École Polytechnique Fédérale de Lausanne, CH-1015 Lausanne, Switzerland*
[7] *Theoretical Chemistry, TU Dresden, Mommsenstr. 13, 01062 Dresden*

(Dated: August 11, 2018)

We present a systematic investigation of the electronic properties of bulk and few layer ReS_2 van der Waals crystals using low temperature optical spectroscopy. Weak photoluminescence emission is observed from two non-degenerate band edge excitonic transitions separated by ~ 20 meV. The comparable emission intensity of both excitonic transitions is incompatible with a fully thermalized (Boltzmann) distribution of excitons, indicating the hot nature of the emission. While DFT calculations predict bilayer ReS_2 to have a direct fundamental band gap, our optical data suggests that the fundamental gap is indirect in all cases.

Emerging transition metal dichalcogenides (TMDs) such as MoS_2, $MoSe_2$, $MoTe_2$, WS_2 and WSe_2 are attracting great attention due to their remarkable electronic properties. In particular, the energy and the character of the band gap can be easily tuned by varying the number of atomic layers in the crystal.[1–5] The two dimensional confinement and reduced dielectric screening in the single and few layer limit result in significantly enhanced exciton and trion binding energies,[6–9] while the lack of inversion symmetry in the monolayer leads to valley-selective optical selection rules.[10–13]

Recently, layered semiconductors with in-plane anisotropy such as black phosphorus,[14,15] and rhenium dichalcogenides (ReX_2, where X stands for Se or S atoms)[16] have joined the family of intensively investigated van der Waals crystals. The sizable in-plane crystal asymmetry results in anisotropic optical,[3,5,17–25] and electrical[17,23,26–28] properties, which can be employed in field effect transistors,[29–32] polarization sensitive photodetectors,[33] and new plasmonic devices.[34] The major advantage of Re dichalcogenides over black phosphorus is their stability under ambient conditions,[35] making them potentially interesting for applications.

Unlike the more extensively studied Mo and W based dichalcogenides, Re based TMDs crystallize in the distorted 1T' structure (schematically shown in Fig. 1(a)) of lower triclinic symmetry.[4,36–38] In rhenium dichalcogenides, two non-degenerate direct excitons couple to light, as observed in the reflectivity contrast and photoluminescence (PL) spectra.[3,5,39] The strong linear polarization of the excitonic transitions provides a new degree of freedom to control the optical response[40,41] of this material. Despite the flurry of recent investigations of the ReS_2 and $ReSe_2$,[16] knowledge about their fundamental electronic properties is extremely limited. For example, the nature of the fundamental band gap remains controversial.

Existing band structure calculations provide no consensus concerning the nature of the fundamental band gap.[4,5,42–44] Studies regarding the absorption edge indicate that both materials have an indirect band gap in the bulk form.[18–21,45] This assignment is supported by recent angle-resolved photoemission spectroscopy (ARPES)[44] and photoemission electron microscopy (PEEM)[43] for the few- and monolayer crystals. However, the observed PL emission[3,5,46] might suggest a direct nature of the band gap in this semiconductor. Intriguingly, a comparable emission intensity is observed from both excitonic states at cryogenic temperatures, despite the fact that they are separated by a few tens of meV.[5] This clearly indicates a strong departure from a thermalized (Boltzmann) exciton distribution, which is expected if the direct excitons are the lowest states.

We have performed a systematic low temperature optical investigation of bulk and few layers ReS_2 combining Raman, PL and reflectivity contrast measurements. Our experimental results support the indirect character of the band gap from bulk down to single layer ReS_2 crystals. The PL has features of hot emission. Their observation, even in the presence of an indirect band gap, is related to the relatively short radiative life time of direct excitons in ReS_2. Although the indirect nature of the gap is generally supported by density functional theory (DFT) band structure calculations, intriguingly, our DFT calculations predict a direct gap for bilayer ReS_2, while experimentally we detect only weak hot emission, characteristic for

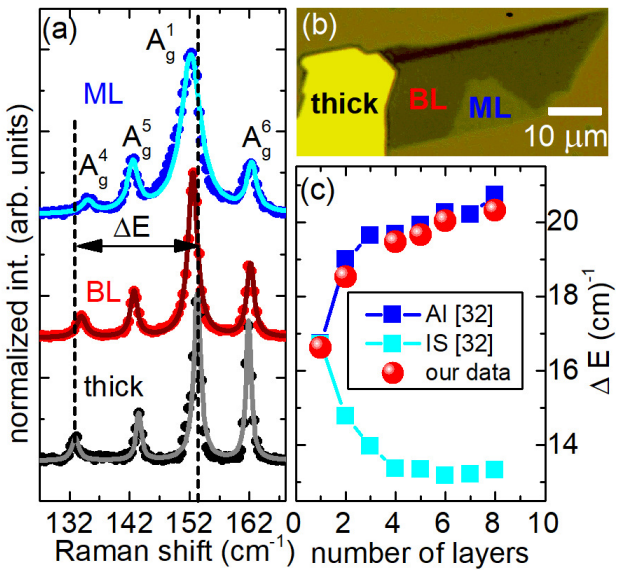

FIG. 1. (a) Representative Raman spectra from monolayer (blue), bilayer (red) and thick (> 8 layers, bulk-like) (black) regions of the ReS_2 flake. The spectra have been normalized with respect to the A_g^1 intensity. We adopt the system used in previous work[47,48] to enumerate Raman modes. (b) Optical image of the investigated ReS_2 flake. (c) Difference $\Delta E = E_{A_g^1} - E_{A_g^4}$ between the A_g^1 and A_g^4 Raman modes as a function of the number of layers. Blue squares show data from literature.[4] Red spheres represent values from our measurements.

the indirect gap.

Mono- and few-layer ReS_2 was obtained from bulk crystals (Hq-graphene) by scotch tape exfoliation onto a surface of degenerately-doped Si covered with a 270 nm thick layer of SiO_2. A flake containing monolayer, bilayer and a thick region (> 8 layers) was selected for the investigation. The flake thickness was confirmed by optical contrast calibrated with Atomic Force Microscopy on flakes of different thicknesses (see Supporting Information). A microscope image of the flake is shown in Fig. 1(b).

Raman measurements were performed in back scattering geometry under ambient conditions, at room temperature, and using a 532 nm laser. The laser light was focused on a spot of approximately 1 μm in diameter using a 100× objective (numerical aperture, NA, 0.9). The spectral resolution of the setup was 0.5 cm^{-1}. The PL and reflectivity contrast measurements were performed in a standard μPL setup in back-scattering geometry, with a long working distance 50× objective having NA=0.55. The sample was excited by CW 532 nm laser for PL or with white light from a tungsten-halogen lamp for reflectivity contrast measurements. The sample was mounted in a helium flow cryostat.

For the density-functional theory (DFT) calculations, all structures were fully optimized (atomic positions and lattice vectors) using the PBE0[49] hybrid exchange-correlation functional, London dispersion interactions as proposed by Grimme,[50] and Gaussian type basis functions (S: all-electron 86-311G* and Re: effective core potential (ECP) with large cores was employed, accounting for scalar relativistic effects) as implemented in Crystal14.[51] Layered materials were built from the bulk 1T' structure of ReS_2, with space group $P\bar{1}$, lattice parameters $a = 6.199$ Å, $b = 6.318$ Å, $c = 6.416$ Å, $\alpha = 118.8°$, $\beta = 91.7°$, $\gamma = 105.5°$, and 12 atoms in the unit cell (4 Re and 8 S). We have used Monkhorst-Pack scheme for k-point mesh during optimization with 3×3×3 and 3×3×1 grid for the bulk and layered systems, respectively. Electronic structure calculations were carried out on the fully optimized structures using PBE[52] exchange-correlation functional, D3 London dispersion interactions,[50] and with Becke and Johnson damping (PBE-D3(BJ)) as implemented in the ADF/BAND package.[53,54] Local basis functions (numerical and Slater-type basis functions of valence triple zeta quality with one polarization function (TZP)) were adopted, and the frozen core approach (small core) was chosen. All calculations included the scalar relativistic corrections within the Zero Order Regular Approximation (ZORA).[55–58] The PBE-D3(BJ) functional underestimates the band gaps, however the band structure shapes and the overall trends with respect to the number of layers should be fairly well represented.

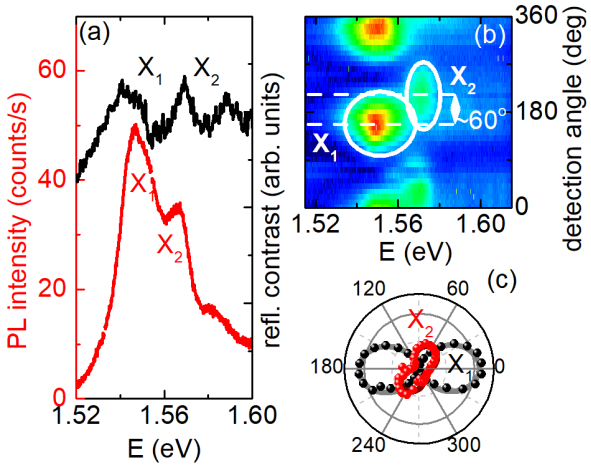

FIG. 2. (a) PL spectrum of bulk-like part of the sample measured at 10 K (red curve) together with the reflection contrast spectrum (black curve). (b) PL spectrum as a function of the linear polarization detection angle. (c) Polar plot of the PL intensity of X_1 (black balls) and X_2 (red balls) excitons as a function of polarization detection angle together with the fitted curves. For clarity points on polar plot are shifted by about 25^o comparing to results presented on (b) panel.

Few-layer ReS_2 can be found in two different polytypes depending on the stacking order referred as isotropic or anisotropic.[4,59] They differ in the relative orientation of the Re-Re bonds in neighboring layers. The number of layers and the stacking order can be determined using

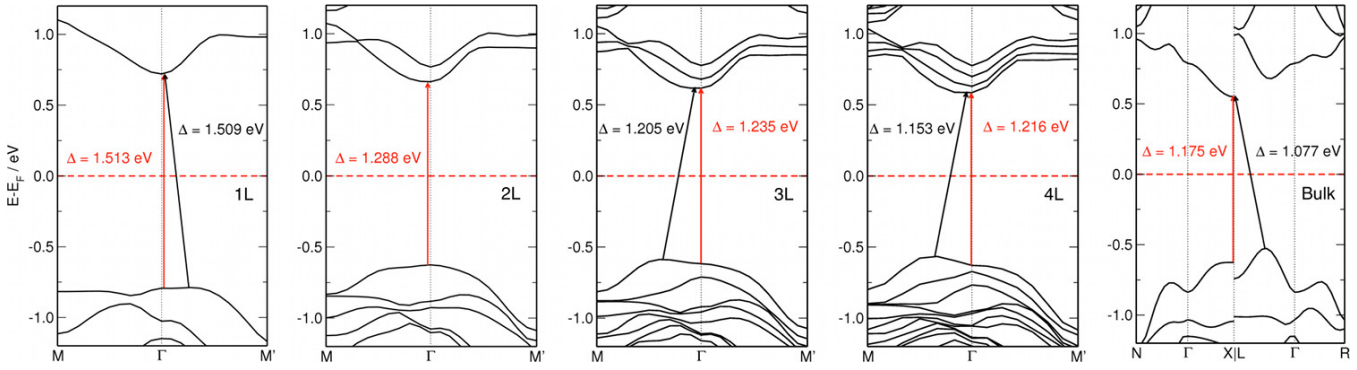

FIG. 3. Calculated DFT band structures of 1T' ReS_2 mono-, few-layer, and bulk. The arrows indicate the optical (red) and the fundamental (black) electronic band gaps.

Raman spectroscopy.[4,48] Fig. 1(a) shows typical Raman spectra measured for different thicknesses of the crystal. The colour coding of the spectra corresponds to that of the labels in the optical image in Fig. 1(b). The pronounced A_g^1 mode at around 155 cm^{-1}, related to the in-plane motion of Re and S atoms, together with lower intensity A_g^4, A_g^5 and A_g^6 are observed in all spectra. The four peaks were fitted with Lorentzian curves to precisely determine the characteristic vibration energy. With decreasing number of layers, the A_g^1 mode softens while the A_g^4 mode hardens. This is characteristic for anisotropic stacking order.[4] Isotropic stacking order shows the opposite trend, *i.e.*, the distance between A_g^1 and A_g^4 mode decreases with increasing thickness. Therefore, the energy separation between A_g^1 and A_g^4 provides a reliable signature of the number of layers. Comparing our data with the previous work (see Fig. 1(c)), we identify areas of monolayer and bilayer thicknesses, together with thicker regions at different positions on the flake.

A typical PL spectrum, collected from a thick part of the crystal, is presented in Fig. 2(a). The two emission peaks at 1.546 eV and 1.566 eV are non-degenerate direct excitonic transitions, previously observed in reflectivity contrast and PL.[3,39,45] The free excitonic nature of these PL peaks is further supported by the reflectivity contrast, which is also plotted in Fig. 2(a). In the reflectivity contrast, both excitonic features are Stokes-shifted by $\simeq$ 10 meV with respect to the PL peaks. The full polarization dependence of the PL spectrum of the bulk-like sample is presented in Fig. 2(b). The emission intensity of both excitons strongly depends on the detection polarization angle, as demonstrated by the polar plot of Fig. 2(c). These data are plotted in a non-polar plot in the Supplementary Information. The variation of the PL intensity with the detection angle shows a characteristic figure of eight dependence in the polar plot. This behavior is well described using $I_0 + I_x \cos^2(\theta + \theta_0)$, from which we extract the angle between the maximum PL intensity for each exciton. In agreement with previous reports,[3,40] the principal polarization axes of the excitons are rotated by $\simeq 60°$ with respect to each other.

To facilitate the interpretation of the optical data, we have performed DFT band structure calculations of the anisotropic ReS_2 crystal with different number of layers, as shown in Fig. 3. The optical gap at the Γ point gradually increases with decreasing number of layers (see also Table 1 in Supporting Information). Intriguingly, the fundamental band gap is predicted to be direct only for the bilayer and becomes again indirect for the monolayer case. Our calculations are in agreement with bulk ReS_2 absorption measurements,[18–21,45] and recent photo-emission electron microscopy (PEEM) and GW calculations.[43] However, the predicted direct nature of the the bilayer ReS_2 is not supported by the PL behavior, as we show in the next paragraphs.

The evolution of the PL spectrum with the flake thickness is presented in Fig. 4(a). As the number of layers decreases, there is a systematic increase of the emission energy, related to the opening of the band gap at the Γ point. The dependence of X_1 and X_2 transition energies versus number of layers is summarized in Fig. 4(b). In our sample, six and four layers thick ReS_2 corresponds to a narrow stripe (see Fig. 1(b)). The PL spectra measured in these regions received some contribution from the bilayer emission, visible around 1.62 eV. The twin-peak PL structure can be consistently observed in all places on our sample with thickness $\geq$ 4 layers (see Fig. 4(a)). The PL emission from monolayer area of the flake was too weak to be observed, consistent with the predicted indirect nature of the gap. For bilayer, the PL spectrum is dominated by a weak, single PL peak attributed to the X_1 exciton, with a weak, high energy shoulder corresponding to the X_2 emission. Given that the X_2 of the bilayer is weak in the unpolarized PL spectrum, we determine its transition energy based on the polarization resolved PL measurements shown in the Supplementary Information. The evolution of the amplitude of the X_1 PL peak with the number of layers is shown in the inset of Fig. 4(a). The emission from the bilayer clearly matches the trend, with no sign of enhanced emission, which is expected to be orders of magnitude stronger if the fundamental gap were direct.

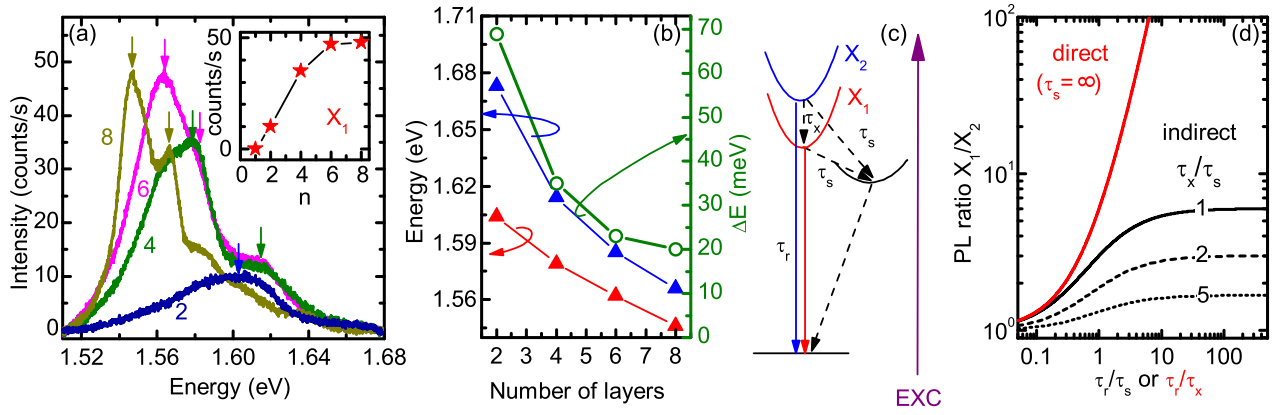

FIG. 4. (a) PL spectra measured at $T = 10\,\mathrm{K}$ for different number of layers. The arrows indicate the position of X_1 and X_2 transitions. The inset shows the amplitude of the X_1 PL as a function of the number of layers n. (b) Dependence of X_1 (red triangles) and X_2 (blue triangles) transition energy as a function of the number of layers and their energy separation. (c) Scheme of carrier relaxation (dashed arrows) and radiative recombination process (red and blue arrows) in the presence of an indirect fundamental gap. (d) Ratio of the X_1 to X_2 PL intensity calculated as function of τ_r/τ_s (or τ_r/τ_x for the direct band gap case with $\tau_s = \infty$) by solving the rate equation model described in the Supplementary Information. For the indirect gap, the ratio was calculated for the three different values of τ_x/τ_s indicated.

The observation of both X_1 and X_2 emissions is at first sight surprising since they are separated by at least 20 meV, which is more than an order of magnitude larger than $k_B T$ at 10 K (~ 0.8 meV). If the exciton population follows a Boltzmann distribution, the intensity ratio between two peaks should be vanishingly small ($\sim 10^{-9}$), *i.e.*, the higher energy X_2 emission should not be observed. The observed PL peaks must arise from hot PL involving emission from excitons which are not fully thermalized. For this to occur, the radiative lifetime must be sufficiently short, compared to the non-radiative relaxation time. In addition, if there is an effective way to depopulate both X_1 and X_2, the intensity of both will be reduced, while the ratio of the intensities will be pushed towards unity. The presence of the indirect band gap below the direct band gap transitions provides such an effective depopulation path. The scheme of the carrier kinetics with the band structure and relaxation paths are indicated schematically in Fig. 4(c). Here, τ_r is the radiative lifetime of the direct excitons, τ_s is the lifetime for scattering to the indirect dark exciton state, and τ_x is the lifetime for scattering from X_2 to X_1. The radiative recombination time of the direct exciton transition is not known for ReS_2. We expect, however, that it lies in the picoseconds time scale, as for other TMDs.[60–62] We estimate that the PL intensity here is $\simeq 2$ orders of magnitude weaker than in direct band gap TMDs. Assuming $\tau_r \simeq 1$ ps, this gives a reasonable ball park figure for the non radiative lifetime $\tau_s \simeq 10$ fs. We have solved the rate equation model to see what conditions should be fulfilled to obtain the observed ratio of X_1 and X_2 PL intensity for the direct and indirect case, which is plotted as a function of τ_r/τ_s in Fig. 4(d) (see Supplementary Information for more details). If the fundamental gap is direct, the ratio of the emission intensities diverges, as expected for $\tau_r/\tau_s > 1$. When the fundamental gap is indirect, for $\tau_r/\tau_s > 1$ the ratio reproduces nicely the experimental observations, saturating between $\simeq 1 - 6$ depending the value of τ_x/τ_s used. For the direct gap, reproducing the X_1 to X_2 intensity ratio observed experimentally would require $\tau_r/\tau_x \leq 1$, which is not expected for semiconductors and incompatible with weak PL. We therefore conclude that the observation of hot PL emission is a smoking gun signature of the indirect gap. Since both excitonic transitions are observed for all thicknesses, we deduce that in all cases the gap is indirect.

To conclude, we have presented a combined low temperature PL and reflectivity contrast investigation of different thicknesses ReS_2 with anisotropic stacking order. The weak PL emission observed from two direct excitons (X_1 and X_2) separated by $\simeq 20$ meV indicates their hot nature, together with the presence of a lower lying indirect band gap. This conclusion is supported by the solution of the rate equations. The weak intensity of the PL, observed for both excitons, is consistently observed down to the bilayer, which points to an indirect fundamental band gap of ReS_2, independent of the number of layers. For bilayer ReS_2, this contradicts the predictions of our DFT calculations, as well as the GW calculations and PEEM investigation found in the literature.[43] However, the difference between optical and fundamental gap is small, as the DFT and GLLB-SC calculations do not include the exciton binding energy.

AUTHOR CONTRIBUTION

Author contributions: DKM and PP coordinated the project. DO fabricated the samples under the supervision of. JMU, DW, A. Suc. and LK performed Raman

spectroscopy measurements. JMU, MB, A. Sur. performed PL and reflectivity contrast measurements. AK, YM performed DFT calculation under TH supervision. JMU, MB, A. Sur., LK, AK, DKM and PP analyzed the data and discussed the results. JMU, MB, AK, DKM, and PP wrote the manuscript with input from all other co-authors.

CONFLICTS OF INTEREST

There are no conflicts of interest to declare.

ACKNOWLEDGMENTS

This work was partially supported by BLAPHENE and STRABOT projects, which received funding from the IDEX Toulouse, Emergence program, "Programme des Investissements d'Avenir" under the program ANR-11-IDEX-0002-02, reference ANR-10-LABX-0037-NEXT, and by the PAN–CNRS collaboration within the PICS 2016-2018 agreement. M.B. appreciates support from the Polish Ministry of Science and Higher Education within the Mobilnosc Plus program (grant no. 1648/MOB/V/2017/0). AK and TH acknowledge funding of Deutsche Forschungsgemeinschaft via the FlagERA project HE 3543/27-1 and ZIH Dresden for providing computational resources.

---

* These authors contributed equally to the work
† paulina.plochocka@lncmi.cnrs.fr

[1] K. F. Mak, C. Lee, J. Hone, J. Shan, and T. F. Heinz, Physical review letters **105**, 136805 (2010).
[2] A. Splendiani, L. Sun, Y. Zhang, T. Li, J. Kim, C.-Y. Chim, G. Galli, and F. Wang, Nano letters **10**, 1271 (2010).
[3] O. B. Aslan, D. A. Chenet, A. M. van der Zande, J. C. Hone, and T. F. Heinz, ACS Photonics **3**, 96 (2016).
[4] X.-F. Qiao, J.-B. Wu, L. Zhou, J. Qiao, W. Shi, T. Chen, X. Zhang, J. Zhang, W. Ji, and P.-H. Tan, Nanoscale **8**, 8324 (2016).
[5] A. Arora, J. Noky, M. Drppel, B. Jariwala, T. Deilmann, R. Schneider, R. Schmidt, O. Del Pozo-Zamudio, T. Stiehm, A. Bhattacharya, P. Krger, S. Michaelis de Vasconcellos, M. Rohlfing, and R. Bratschitsch, Nano Letters **17**, 3202 (2017).
[6] K. F. Mak, K. He, C. Lee, G. H. Lee, J. Hone, T. F. Heinz, and J. Shan, Nature materials **12**, 207 (2013).
[7] J. S. Ross, S. Wu, H. Yu, N. J. Ghimire, A. M. Jones, G. Aivazian, J. Yan, D. G. Mandrus, D. Xiao, W. Yao, *et al.*, Nature communications **4**, 1474 (2013).
[8] A. Chernikov, T. C. Berkelbach, H. M. Hill, A. Rigosi, Y. Li, O. B. Aslan, D. R. Reichman, M. S. Hybertsen, and T. F. Heinz, Physical review letters **113**, 076802 (2014).
[9] K. He, N. Kumar, L. Zhao, Z. Wang, K. F. Mak, H. Zhao, and J. Shan, Physical review letters **113**, 026803 (2014).
[10] D. Xiao, G.-B. Liu, W. Feng, X. Xu, and W. Yao, Physical Review Letters **108**, 196802 (2012).
[11] K. F. Mak, K. He, J. Shan, and T. F. Heinz, Nature nanotechnology **7**, 494 (2012).
[12] H. Zeng, J. Dai, W. Yao, D. Xiao, and X. Cui, Nature nanotechnology **7**, 490 (2012).
[13] X. Xu, W. Yao, D. Xiao, and T. F. Heinz, Nature Physics **10**, 343 (2014).
[14] F. Xia, H. Wang, and Y. Jia, Nature communications **5**, 4458 (2014).
[15] A. Carvalho, M. Wang, X. Zhu, A. S. Rodin, H. Su, and A. H. C. Neto, Nature Reviews Materials **1**, 16061 (2016).
[16] M. Hafeez, L. Gan, A. S. Bhatti, and T. Zhai, Materials Chemistry Frontiers (2017).
[17] C. Ho, M. Hsieh, C. Wu, Y. Huang, and K. Tiong, Journal of Alloys and Compounds **442**, 245 (2007).
[18] C. H. Ho, Y. S. Huang, K. K. Tiong, and P. C. Liao, Physical Review B **58**, 16130 (1998).
[19] K. Friemelt, M. LuxSteiner, and E. Bucher, Journal of Applied Physics **74**, 5266 (1993).
[20] C. H. Ho, P. C. Liao, Y. S. Huang, T. R. Yang, and K. K. Tiong, Journal of Applied Physics **81**, 6380 (1997).
[21] C. Liang, Y. Chan, K. Tiong, Y. Huang, Y. Chen, D. Dumcenco, and C. Ho, Journal of Alloys and Compounds **480**, 94 (2009).
[22] D. Wolverson, S. Crampin, A. S. Kazemi, A. Ilie, and S. J. Bending, Acs Nano **8**, 11154 (2014).
[23] Q. Cui, J. He, M. Z. Bellus, M. Mirzokarimov, T. Hofmann, H.-Y. Chiu, M. Antonik, D. He, Y. Wang, and H. Zhao, Small **11**, 5565 (2015).
[24] Y. Cui, F. Lu, and X. Liu, Scientific Reports **7**, 40080 (2017).
[25] D. A. Chenet, O. B. Aslan, P. Y. Huang, C. Fan, A. M. van der Zande, T. F. Heinz, and J. C. Hone, Nano Letters **15**, 5667 (2015).
[26] C. H. Ho, Y. S. Huang, K. K. Tiong, and P. C. Liao, Journal of Physics: Condensed Matter **11**, 5367 (1999).
[27] Y.-C. Lin, H.-P. Komsa, C.-H. Yeh, T. Bjrkman, Z.-Y. Liang, C.-H. Ho, Y.-S. Huang, P.-W. Chiu, A. V. Krasheninnikov, and K. Suenaga, ACS Nano **9**, 11249 (2015), pMID: 26390381, http://dx.doi.org/10.1021/acsnano.5b04851.
[28] K. Tiong, C. Ho, and Y. Huang, Solid state communications **111**, 635 (1999).
[29] S. Yang, S. Tongay, Y. Li, Q. Yue, J.-B. Xia, S.-S. Li, J. Li, and S.-H. Wei, Nanoscale **6**, 7226 (2014).
[30] C. M. Corbet, C. McClellan, A. Rai, S. S. Sonde, E. Tutuc, and S. K. Banerjee, ACS nano **9**, 363 (2014).
[31] C. M. Corbet, S. S. Sonde, E. Tutuc, and S. K. Banerjee, Applied Physics Letters **108**, 162104 (2016).
[32] D. Ovchinnikov, F. Gargiulo, A. Allain, D. J. Pasquier, D. Dumcenco, C.-H. Ho, O. V. Yazyev, and A. Kis, Nature

communications **7** (2016).
[33] E. Zhang, P. Wang, Z. Li, H. Wang, C. Song, C. Huang, Z.-G. Chen, L. Yang, K. Zhang, S. Lu, *et al.*, ACS nano **10**, 8067 (2016).
[34] T. Low, R. Roldán, H. Wang, F. Xia, P. Avouris, L. M. Moreno, and F. Guinea, Physical review letters **113**, 106802 (2014).
[35] A. Favron, E. Gaufrès, F. Fossard, A.-L. Phaneuf-LHeureux, N. Y. Tang, P. L. Lévesque, A. Loiseau, R. Leonelli, S. Francoeur, and R. Martel, Nature materials **14**, 826 (2015).
[36] H. Murray, S. Kelty, R. Chianelli, and C. Day, Inorganic Chemistry **33**, 4418 (1994).
[37] S. P. Kelty, A. F. Ruppert, R. R. Chianelli, J. Ren, and M.-H. Whangbo, Journal of the American Chemical Society **116**, 7857 (1994).
[38] S. Tongay, H. Sahin, C. Ko, A. Luce, W. Fan, K. Liu, J. Zhou, Y.-S. Huang, C.-H. Ho, J. Yan, D. F. Ogletree, S. Aloni, J. Ji, S. Li, J. Li, F. M. Peeters, and J. Wu, Nature Communications **5** (2014), 10.1038/ncomms4252.
[39] Y. S. Huang, C. H. Ho, P. C. Liao, and K. K. Tiong, Journal of alloys and compounds **262**, 92 (1997).
[40] S. Sim, D. Lee, M. Noh, S. Cha, C. H. Soh, J. H. Sung, M.-H. Jo, and H. Choi, Nature Communications **7**, 13569 (2016).
[41] S. Sim, D. Lee, A. V. Trifonov, T. Kim, S. Cha, J. H. Sung, S. Cho, W. Shim, M.-H. Jo, and H. Choi, Nature Communications **9**, 351 (2018).
[42] H.-X. Zhong, S. Gao, J.-J. Shi, and L. Yang, Physical Review B **92** (2015), 10.1103/PhysRevB.92.115438.
[43] M. Gehlmann, I. Aguilera, G. Bihlmayer, S. Nemk, P. Nagler, P. Gospodari, G. Zamborlini, M. Eschbach, V. Feyer, F. Kronast, E. Myczak, T. Korn, L. Plucinski, C. Schller, S. Blgel, and C. M. Schneider, Nano Letters **17**, 5187 (2017).
[44] J. L. Webb, L. S. Hart, D. Wolverson, C. Chen, J. Avila, and M. C. Asensio, Physical Review B **96**, 115205 (2017), arXiv:1704.06042.
[45] S. J. Zelewski and R. Kudrawiec, Scientific Reports **7**, 15365 (2017).
[46] I. Gutiérrez-Lezama, B. A. Reddy, N. Ubrig, and A. F. Morpurgo, 2D Materials **3** (2016), 10.1088/2053-1583/3/4/045016.
[47] Y. Feng, W. Zhou, Y. Wang, J. Zhou, E. Liu, Y. Fu, Z. Ni, X. Wu, H. Yuan, F. Miao, B. Wang, X. Wan, and D. Xing, Physical Review B **92** (2015), 10.1103/PhysRevB.92.054110.
[48] A. McCreary, J. R. Simpson, Y. Wang, D. Rhodes, K. Fujisawa, L. Balicas, M. Dubey, V. H. Crespi, M. Terrones, and A. R. Hight Walker, Nano Letters (2017), 10.1021/acs.nanolett.7b01463.
[49] J. P. Perdew, M. Emzerhof, and K. Burke, Journal Of Chemical Physics **105**, 9982 (1996).
[50] S. Grimme, J. Comp. Chem. **27**, 1787 (2006).
[51] R. Dovesi, V. R. Saunders, C. Roetti, R. Orlando, C. M. Zicovich-Wilson, F. Pascale, B. Civalleri, K. Doll, N. M. Harrison, I. J. Bush, P. D'Arco, M. Llunell, M. Causà, and Y. Noël, "Crystal14 user's manual (university of torino, torino, 2014)." (CRYSTAL14 User's Manual (University of Torino, Torino, 2014).).
[52] J. P. Perdew, K. Burke, and M. Ernzerhof, Phys. Rev. Lett. **77**, 3865 (1996).
[53] G. te Velde and E. J. Baerends, Phys. Rev. B **44**, 7888 (1991).
[54] P. Philipsen, G. te Velde, E. Bearends, J. Berger, P. de Boeij, J. Groenveld, E. Kadantsev, R. Klooster, F. Kootstra, P. Romaniello, D. Skachkov, J. Snijders, G. Wiesnekker, and T. Ziegler, "Band2014, scm, theoretical chemistry, vrije universiteit, amsterdam, netherlands," (2014).
[55] P. H. T. Philipsen, E. van Lenthe, J. G. Snijders, and E. J. Baerends, Phys. Rev. B **56**, 13556 (1997).
[56] E. van Lenthe, E. J. Baerends, and J. G. Snijders, The Journal of Chemical Physics **99**, 4597 (1993).
[57] E. van Lenthe, A. Ehlers, and E.-J. Baerends, The Journal of Chemical Physics **110**, 8943 (1999).
[58] M. Filatov and D. Cremer, Molecular Physics **101**, 2295 (2003).
[59] L. Hart, S. Dale, S. Hoye, J. L. Webb, and D. Wolverson, Nano Letters **16**, 1381 (2016).
[60] T. Godde, D. Schmidt, J. Schmutzler, M. Aßmann, J. Debus, F. Withers, E. Alexeev, O. Del Pozo-Zamudio, O. Skrypka, K. Novoselov, *et al.*, Physical Review B **94**, 165301 (2016).
[61] C. Robert, D. Lagarde, F. Cadiz, G. Wang, B. Lassagne, T. Amand, A. Balocchi, P. Renucci, S. Tongay, B. Urbaszek, *et al.*, Physical Review B **93**, 205423 (2016).
[62] C. Robert, T. Amand, F. Cadiz, D. Lagarde, E. Courtade, M. Manca, T. Taniguchi, K. Watanabe, B. Urbaszek, and X. Marie, Physical Review B **96**, 155423 (2017).